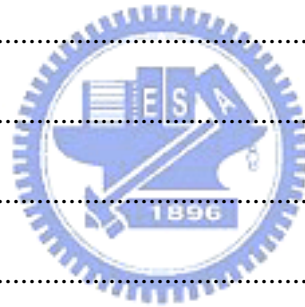


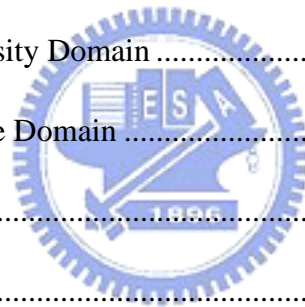
Contents

中文摘要	i
English Abstract	iv
誌謝	vii
Table of Contents	viii
List of Tables	xi
List of Figures	xii
Chapter 1 Introduction.....	1
Chapter 2 Background	9
2.1 Boundary-Based Methods.....	9
2.1.1 Chain Code.....	10
2.1.2 Signature	11
2.2 Region-Based Methods.....	12
2.2.1 Quadtree decomposition	12
2.2.2 Polygon approximation.....	13
2.3 Transform-Based Methods.....	13
2.4 Multi-resolution-Based Methods	14
2.4.1 Gaussian pyramid and Laplacian pyramid decompositions.....	15
2.4.2 Wavelet-based methods.....	16
2.5 Fractal-Based Methods	17
2.6 Recent Works	18



Chapter 3 Verge Point Extraction and Image Surface Reconstruction	23
3.1 Extracting Verge Points on One-Dimensional Profiles.....	23
3.2. Extracting Verge Points on Image Surfaces.....	28
3.2.1. Verge Points Extraction Based on Principal Curvature	28
3.2.2. Quantitative Comparisons between Matrix M and Hessian H	32
3.2.3. Curvature Threshold Determination	45
3.3. Image Surface Reconstruction	48
3.3.1. Surface Reconstruction for Gray-Scale Images.....	48
3.3.2. Surface Reconstruction for Color Images.....	57
Chapter 4 Data Structures Based on Verge Point Representation	61
4.1. Verge Curves Linking	61
4.2. B-spline Curve Approximation.....	63
4.3. Image Compression Based on Verge Point Representation.....	71
4.3.1. Data Arrangement for the Proposed Image Codec	73
4.3.2. Quantizers Selections.....	75
4.3.2.1. Curvature Quantizer Q_k	75
4.3.2.2. Shape Qunatizer Q_d	77
4.3.2.3. Intensity Qunatizer Q_i	79
4.3.3. Entropy Coding.....	80
4.4. Scalable Image Transmission.....	87
4.4.1 SNR scalability	87
4.4.2 Spatial Scalability	91
4.4.3 Shape Scalability.....	94

4.5 Interactive Image Transmission	95
Chapter 5 Image Features Detection and Image Surface Manipulation ...	98
5.1. Image Features Detection	98
5.1.1. Point Detection.....	99
5.1.2. Line Edge Detection	101
5.1.3. Step Edge Detection.....	103
5.1.4. Corner Detection.....	109
5.1.5. Homogeneous Region Detection	112
5.2. Image Surface Manipulation.....	116
5.2.1. Problem Formulation	117
5.2.2. Editing Images in Intensity Domain	120
5.2.3. Editing Images in Shape Domain	130
Chapter 6 Conclusions.....	133
Bibliography	137
Appendix.....	143
Publication	147
簡歷.....	149



List of Tables

Table 3.1 SNR comparisons between A and H. 44

Table 3.2 (Test images: Lena, Fruit, Peppers.)..... 55

Table 4.1 The number of required verge points and the MSE under different Tk's.
..... 76

Table 4.2 Relation between allowed shape distortion Ad and required control points.
..... 78

Table 4.3. Code words for body control points..... 82

Table 4.4. (a) Experimental results. (b) Resource consumption. 85

Table 4.5. Average required execution time and corresponding bitstream size... 85



List of Figures

Fig. 1.1. Illustration of image surface	3
Fig. 1.2 Concept of the proposed method in one-D profile	4
Fig. 1.3 Overview of the proposed image representation scheme	5
Fig. 2.1. Illustration of 4-connected grid and 8-connected grid.....	10
Fig. 2.2. Examples of chain code. (a) Digital boundary. (b) 4-connected chain code. (c) 8-connected chain code.....	10
Fig. 2.3. An example of signature representation for objects with different shapes.	11
Fig. 2.4. Concept of quadtree. (a) Partitioned image. (b) Quadtree representation.	12
Fig. 2.5. Examples of transform-based methods. (a) Original image. (b) DFT transform. (c) DCT transform.	14
Fig. 2.6. Example of Gaussian pyramid and Laplacian pyramid.....	15
Fig. 2.7. Architecture of image decomposition and reconstruction using Laplacian pyramid.	16
Fig. 2.8. An example of wavelet decomposition with a 3-layer hierarchy	17
Fig. 2.9 Feature extraction by dilation gradient and erosion gradient	21
Fig. 3.1. Concept of verge points. (a) Illustration of P_e and \vec{e}_i . (b) Reconstructed profile with correct pulley parameters. (c) Reconstructed profile with the sign of the right pulley being incorrectly recorded. (d) Reconstructed profile with the position of the right pulley being incorrectly recorded. (e) Reconstructed profile with the radius of the right pulley being incorrectly recorded.....	25
Fig. 3.2. Enhancement using verge points. (a) Original profile. (b) Edge enhancement. (c) Contrast enhancement.	28
Fig. 3.3. Image surface emulation using a rubber cloth and pipes. (a) Synthetic image.	

(b) Corresponding image surface of (a). (c) Illustration of a rubber cloth stretched by pipes. 29

Fig. 3.4. Comparisons between **A** and **H**, in terms of SNR performance. (a) Step edge image polluted by white Gaussian noise with $\sigma_n = 2$. (b) A transversal profile of (a). (c) Computed curvature profile based on Matrix **A**. (d) Computed curvature profile based on Hessian **H**..... 32

Fig. 3.5. (a) Expected $|k|$ profile without noise interference (cyan) and the standard deviation of $|\Delta k|$ (pink and yellow), based on Matrix **A**. (b) Expected $|\hat{k}|$ profile without noise interference (red) and the standard deviation of $|\Delta \hat{k}|$ (green and blue), based on Hessian **H**. (Remark: $\sigma_m = 1, \sigma_n = 2$ for this simulation). 41

Fig. 3.6. (a) Expected $|k|$ profile without noise interference (cyan) and the standard deviation of $|\Delta k|$ (pink and yellow), based on Matrix **A**. (b) Expected $|\hat{k}|$ profile without noise interference (red) and the standard deviation of $|\Delta \hat{k}|$ (green and blue), based on Hessian **H**. (Remark: $\sigma_m = 1, \sigma_n = 3$ for this simulation). 42

Fig. 3.7. (a) Expected $|k|$ profile without noise interference (cyan) and the standard deviation of $|\Delta k|$ (pink and yellow), based on Matrix **A**. (b) Expected $|\hat{k}|$ profile without noise interference (red) and the standard deviation of $|\Delta \hat{k}|$ (green and blue), based on Hessian **H**. (Remark: $\sigma_m = 2, \sigma_n = 3$ for this simulation). 43

Fig. 3.8. (a) Reconstructed image using direct linear interpolation. (b)~(f) Reconstructed images in the first few iterations of the iterative linear interpolation. (g) Final result using iterative linear interpolation. (h) The difference image between the original image and the reconstructed image in (g)..... 47

Fig. 3.9. (a) Reconstructed image using direct linear interpolation. (b)~(f) Reconstructed images in the first few iterations of the iterative linear interpolation. (g) Final result using iterative linear interpolation. (h) The difference image between

the original image and the reconstructed image in (g). (i) Contrast sensitivity function of human visual system. (j) Original image surface around shoulder. (k) Reconstructed image surface around shoulder. (l) Original image surface around hair. (m) Reconstructed image surface around hair. 53

Fig. 3.10. (a) Original image. (b) Extracted verge points. (c) Reconstructed image. 54

Fig. 3.11. (a) Comparison of reconstructed images. The intensity values at the verge points are quantized into 2, 4, 8, 16, 32, 64, 128, and 256 levels, respectively (from upper-left to lower-right). (b) The PSNR value of these reconstructed images... 56

Fig. 3.12. (a) Original color image (256×256). (b) Reconstructed color image under CIE L*a*b* color space, using 16812 verge points for L*, 12537 verge points for a*, and 14416 verge points for b*. 58

Fig. 3.13. (a) Original color image (256×256). (b) Reconstructed color image under CIE L*a*b* color space, using 15723 verge points for L*, 11435 verge points for a*, and 13429 verge points for b*. 59

Fig. 3.14. (a) Reconstructed color image under CIE L*a*b* color space, using 34613 verge points for L*, 39961 verge points for a*, and 28452 verge points for b*. (b) Reconstructed color image under CIE L*a*b* color space, using 34613 verge points for L*, 28442 verge points for a*, and 19875 verge points for b*..... 60

Fig. 4.1 (a) Original image. (b) Eigenvectors $\Lambda_2(x, y)$ around Lena's shoulder. 63

Fig. 4.2. B-spline approximation. (a) Shape component (C: shape control points, k: knots). (b) Intensity component (I: intensity control points, k: knots). 64

Fig. 4.3. (a) Original image. (b) Original image surface. (c) Extracted verge curves. (d) Control points using B-spline approximation. (e) Reconstructed image surface using (d). (f) Reconstructed image. 66

Fig. 4.4. (a) Reconstructed gray-level image using B-spline approximation. (2957 control points) (b) Reconstructed color image using B-spline approximation under the CIE L*a*b* color space. (L*: 3173 control points, a*: 2783 control points, b*: 2974 control points). 67

Fig. 4.5. (a) Number of verge points versus the threshold of curve length. (b) PSNR of the reconstructed images versus the threshold of curve length (using verge-curve representation). (c) Number of control points versus the threshold of curve length. (d)

PSNR of the reconstructed image versus the threshold of curve length (using B-spline control-point representation). (e) Ratio of the total pixel number over the number of verge points. (f) Ratio of the total pixel number over the number of control points. 70

Fig. 4.6. Block diagram of JPEG encoder..... 71

Fig. 4.7. Block diagram of the proposed image codec..... 73

Fig. 4.8. Data structure for the storage of verge curves. 74

Fig. 4.9 Basic data structure for B-spline representation..... 74

Fig. 4.10. (a) Original image. (b) Extracted verge points with $T_k=3$. (c) Extracted verge points with $T_k=6$. (d) Extracted verge points with $T_k=9$ 75

Fig. 4.11. Estimated rate-distortion curve of the image “peppers”..... 77

Fig. 4.12. (a) Allowed position distortion $A_d=1$. (b) Allowed position distortion $A_d=3$ 78

Fig. 4.13. Adaptive Q_i determination for the image “peppers”..... 80

Fig. 4.14. (a) Two-level sequential scan. (b) Statistics of run length. (c) Statistics of position x. (d) Statistics of position y..... 81

Fig. 4.15. (a) Approximated B-spline curves, where curves with positive and negative curvature values are indicated in red and green respectively. (b) Decoded Image using the proposed method. (c) Decoded Image using JPEG. 83

Fig. 4.16. Illustrations of two different compression algorithms. (a) Reconstructed image using the proposed method; compression rate=31.12, PSNR=28.67. (b) Reconstructed image using JPEG compression, compression rate=31.08, PSNR=30.65. 84

Fig. 4.17. (a) The relation between storage requirement and PSNR for different T_k 's, based on the verge curve representation. (Test image: 512x512 Lena image.) (b) The relation between storage requirement and PSNR for different T_k 's, based on the B-spline curve representation. (Test image: 512x512 Lena image.) 86

Fig. 4.18. Progressive image reconstruction. (a) Using “top-layer” verge curves only; totally 8219 verge points. (b) Using “top-layer” and “middle-layer” verge curves; totally 11523 verge points. (c) Using all verge curves; totally 15926 verge points.

.....	89
Fig. 4.19. Data arrangement for SNR scalable transmission.	90
Fig. 4.20. SNR scalable transmission of the image “peppers”. (a) (CS,b ₁). (b) (CS+MS,b ₂). (c) (CS+MS+FS,b ₃).....	91
Fig. 4.21. Decoding process for the proposed spatial scalability scheme.....	92
Fig. 4.22 Spatial scalable transmission for the image “peppers”. (a) 256x256. (b) 370x370. (c) 512x512.	93
Fig. 4.23. Data arrangement for shape scalability.....	94
Fig. 4.24. Examples of shape scalability. (a) S1. (b) S1+S2. (c) S1+S2+S3.	95
Fig. 4.25. Examples of feature-of-interest selection and transmission. (a) Original decoded image. (b) Features selected for bitplane shifting. (c) Decoded image with bitplane shifting. (d) Features selected for resolution shifting. (e) Decoded image using (d).	97
Fig. 5.1 (a) Original image. (b) Detected edges.....	99
Fig. 5.2 Point detection (a) Original point image. (b) Point image after Gaussian smoothing. (c) Point image surface. (d) Larger eigenvalues, k ₁ . (e) Smaller eigenvalues, k ₂	100
Fig. 5.3 Ridge Detection (a) Original ridge image. (b) Ridge image after Gaussian smoothing. (c) Ridge image surface. (d) Larger eigenvalues, k ₁ . (e) Smaller eigenvalues, k ₂	101
Fig. 5.4 Valley detection. (a) Original valley image. (b) Valley image after Gaussian smoothing. (c) Valley image surface. (d) Larger eigenvalues, k ₁ . (e) Smaller eigenvalues, k ₂	102
Fig. 5.5. Step edge detection. (a) Original step edge. (b) Step edge after Gaussian smoothing. (c) Step edge image surface. (d) Larger eigenvalues, k ₁ . (e) Smaller eigenvalues, k ₂ . (f) Eigenvector, $\Lambda_1(x, y)$. (g) Eigenvector, $\Lambda_2(x, y)$	103
Fig. 5.6. (a) Illustration of edge center, edge span, and edge contrast. (b) Concept of using verge points to detect edges.	105
Fig. 5.7 Edge strength determination.....	105

Fig. 5.9. (a) Original image. (b) Detected edges using the proposed method. (c) Detected edges using the Canny Operator.	106
Fig. 5.10. (a) Original image. (b) Detected edges using the proposed method. (c) Detected edges using the Canny Operator.	107
Fig. 5.11. (a) Original edge image. (b) Positions of the detected high-curvature pair under different scales. (c) Reconstructed edge images using the detected edge center, edge contrast, and edge span for different scales.....	108
Fig. 5.12 Corner detection (a) A Corner image. (b) Corner image after Gaussian smoothing. (c) Image surface around corners. (d) Larger eigenvalues, k_1 . (e) Smaller eigenvalues, k_2 . (f) Another type of corner. (g) Larger eigenvalues, k_1 . (h) Smaller eigenvalues, k_2	109
Fig. 5.13. (a) Concept of corner detection. (b) Detected corners using Hessian \mathbf{H} . (c) Detected corners using Harris operator.....	111
Fig. 5.14. Fingertips detection.	112
Fig. 5.15. (a) Original images. (b) Feature map. (c) First level region map. (d) Second level region map. (e) Third level region map. (f) Multi-level region map. (g) Final region segmentation.....	114
Fig. 5.16. (a) Original images. (b) Multi-level region map. (c) Final region segmentation.	115
Fig. 5.17. Concept of image decomposition.	118
Fig. 5.18. (a) Original image. (b) Extracted verge points. (c) Skeleton component with threshold $T_k = 6$. (d) Residual component of Fig. 4.13(c). (e) Enhancing skeleton component only. (f) Changing residual component only; α is set as 0.5.....	120
Fig. 5.19. (a) Original image. (b) Enhanced image using proposed method. (c) Enhanced image using histogram equalization. (d)-(f) Histograms of (a)-(c) respectively.	122
Fig. 5.20. Image contrast and sharpness altering. (a) Image with original contrast. (b) Image with enhanced contrast. (c) Image with softened contrast. (d) Edge enhancement.	123
Fig. 5.21 (a) Original image. (b) Enhanced color image by enhancing the L	

component only.....	124
Fig. 5.22. Verge points extracted from Fig. 5.18(a) with length threshold = 50 pixels.	124
Fig. 5.23. (a) Original image. (b) Enhancing long features only. (c) Enhancing short features only.....	126
Fig. 5.24. (a) Original image. (b) Image of (a) after histogram equalization. (c) Histogram of (a). (d) Histogram of (b). (e) Interactive skeleton curves grouping. (f) Selected skeleton curves. (g) Image editing using the proposed method.	129
Fig. 5.25. (a) Original Image. (b) Interactive editing.....	129
Fig. 5.26. (a) Original image. (b) Example of feature removals. (c) Example of feature creations.....	131
Fig. 5.27. Interactive shape editing. (a) Original image. (b) Original control points. (c) Modified control points. (d) Influenced zone. (e) Modified image.	132
Fig. 5.28. Illustrations of image manipulations using verge points. (a) Image editing by changing the gray level of a region at the lower-right corner. (b) Image editing by changing the shape of mouth and the shape of a region at the lower-right corner.	132